Hindawi
Mathematical Problems in Engineering
Volume 2022, Article ID 7086885, 9 pages
https://doi.org/10.1155/2022/7086885

Research Article

Research on SDH Model Calibration Algorithm for Robotic Arm Based on Differential Transform

Zhaole Wang, Yaqiu Liu, and Lina Liu

Department of Information and Computer Engineering, Northeast Forestry University, Harbin, Heilongjiang 150000, China

Correspondence should be addressed to Yaqiu Liu; darling@nefu.edu.cn

Received 28 April 2022; Accepted 22 June 2022; Published 31 July 2022

Academic Editor: Xiantao Jiang

With the development of science and technology, it has had a great impact on the manufacturing industry. The manufacturing industry has higher and higher requirements for industrial manipulators, and the expectations for the quality and function of the industrial manipulators in the manufacturing industry are increasing day by day. At the same time, the requirements for the working accuracy of the manipulators are also getting higher and higher. In this paper, a new method is proposed. An error compensation and calibration algorithm based on parameter separation and integration of the standard DH model (SDH) is used to construct the kinematic model of the manipulator. The six groups of structural parameters of the six-axis manipulator are calibrated once every two groups, thereby eliminating the influence of the singular value of the position of the manipulator. Finally, the feasibility of this scheme is verified by simulation experiments, the accuracy is ensured, and the expected purpose is achieved. Because the method in this paper has high requirements on the posture of the manipulator, it reduces the overall calibration calculation and saves time, which has a certain effect on the improvement of the industrial manipulator in the manufacturing industry.

1. Introduction

Because of the complexity of industrial manipulator components, it is necessary to conduct in-depth research on them so as to realize the effective operation and control of the manipulator on the basis of mastering the relevant content. The actual accuracy and theoretical design model of the manipulator body may be inaccurate. In order to ensure that the manipulator body conforms to the theoretical design model, improves the positioning and trajectory accuracy of the manipulator, or can completely move according to the program, the manipulator needs to be calibrated after assembly. The accuracy of the kinematic model can be improved if all deviations are reflected in the DH parameters.

The main sources of kinematic error in robotic arms include machining error, assembly error, zero-point error, reducer return, reduction ratio error, and calibration error, of which calibration error is limited by the rudimentary calibration device and the streamlined calibration process, and in fact, the largest errors often come from this area.

The above calibration methods have two shortcomings: one is that the established robotic arm models are mostly MDH models, which adds an extra parameter to be calibrated, i.e., increases the difficulty of calibration. In this paper, an error compensation scheme based on the standard DH model is proposed to address these two problems in the error calibration process. The traditional standard DH model has the drawback that when two adjacent axes of the arm are parallel or nearly parallel, small errors can cause large changes in the DH structural parameters, resulting in oddities in the arm's position and even damage to the arm. Noting that the differential transformation matrix of the standard DH model is only related to fixed parameters, such as the linkage deflection and linkage rotation angle, and not the joint angle, this greatly simplifies the calculation of the error calibration.

In this paper, a new error calibration and compensation model are developed by making appropriate improvements to the standard DH model, which in turn solves this problem well.

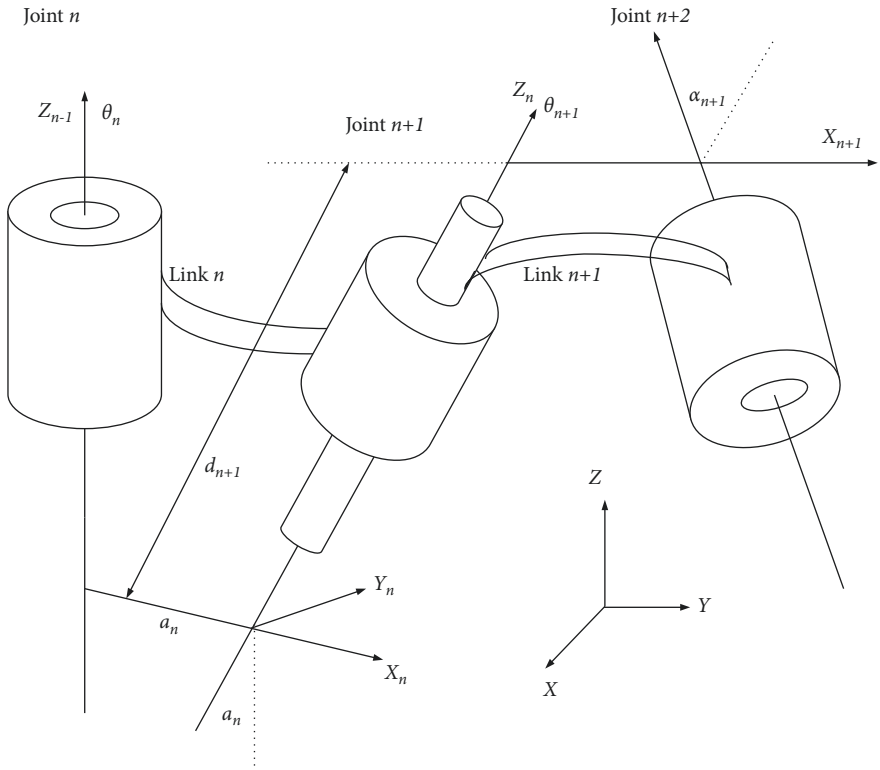

Figure 1: Schematic diagram of the standard DH model of a robotic arm.

2. Kinematic Model of a Robotic Arm

During the movement of a robot arm, the angles of the joints of the arm need to be adjusted to achieve the corresponding Cartesian spatial position, and the matrix characterizing this type of transformation relationship is called the mechanical Jacobi matrix. The mechanical Jacobi matrix is only related to the *D-H* parameters of the arm itself and varies from arm to arm. Suppose a joint is fixed and, without any constraints, the joints adjacent to it have six freely changeable dimensions in free space (Cartesian space) with respect to the fixed joint, i.e., six degrees of freedom; if an independent coordinate system is established for each joint, then the method of flush coordinate transformation is sufficient to solve the problem. However, this is not a good representation of a chain arm system with a unique structure rather than a simple free rigid body, nor is it possible to relate the property parameters of the joints themselves (rotation angle for rotating joints, translation distance for translating joints) to the coordinate transformation.

When expressing the transformation relationship between two coordinate systems, a rotation matrix R and a displacement matrix P are usually required, with a total of 12 parameters. For traditional manipulators, the transformation relationship between coordinate systems can be clearly represented by four parameters θ, d, a, and α, provided that the following two constraints are satisfied. θn represents the axis Xn and axis $Xn-1$, dn represents the directional distance between the axis $Xn-1$ and axis Xn along the positive direction of the axis $Zn-1$, an represents the directional distance between the axis $Zn-1$ and axis Zn along the positive direction of the axis X, and α represents axis angle between $Zn-1$ and axis Zn. a is the directional distance between the $Zn-1$ axis and Zn axis along the Xn axis, and α is the angle between the $Zn-1$ axis and Zn axis. The specific positional relationship and direction of the parameters are shown in Figure 1.

As can be seen in Figure 1, the transformation of the coordinate system O_{n-1} to the coordinate system O_n needs to be done in four steps, first, rotating the coordinate system O_{n-1} around Z_{n-1} by an angle of θ_n, translating along the positive direction of Z_{n-1} by the length of d_n, then translating along the positive direction of X_n by the length of d_n, and finally rotating around X_n by an angle of α_n

Let A_n denote the transformation matrix from the coordinate system O_{n-1} to the coordinate system O_n, then A_n can be expressed as follows:

$$\begin{aligned} A_n &= Rot\left(Z_{n-1,}\theta_n\right) * Trans\left(Z_{n-1,}d_n\right) * Trans\left(X_{n-1,}a_n\right) \\ &\quad * Rot\left(X_{n-1,}\alpha_n\right) \\ &= \begin{bmatrix} c\theta_n & -s\theta_n c\alpha_n & s\theta_n s\alpha_n & a_n c\theta_n \\ s\theta_n & c\theta_n c\alpha_n & -c\theta_n s\alpha_n & a_n s\theta_n \\ 0 & s\alpha_n & c\alpha_n & d_n \\ 0 & 0 & 0 & 1 \end{bmatrix}, \end{aligned} \tag{1}$$

where $c\theta_n$ denotes $\cos\theta_n$, $s\theta_n$ denotes $\sin\theta_{n.}$ ... and so on. The symbols of this type in the equations that indicate the same meaning and are not repeated.

The transformation matrix of the 6-axis robot arm is the transformation matrix of each joint multiplied together in order, and by substituting (1), we get

$$
\begin{aligned}
{}^{0}_{6}T &= A_1 * A_2 * A_3 * A_4 * A_5 * A_6 \\
&= \begin{bmatrix} f_{11} & f_{12} & f_{13} & p_1 \\ f_{21} & f_{22} & f_{23} & p_2 \\ f_{31} & f_{32} & f_{33} & p_3 \\ 0 & 0 & 0 & 1 \end{bmatrix}.
\end{aligned} \tag{2}
$$

2.1. Calibration Algorithm for Errors in the Structural Parameters of the Robot Arm. The inverse kinematics of a manipulator is the calculation of the angular values of the joints of the manipulator from the known coordinate positions or poses of the end-effectors, also known as the inverse kinematics of the manipulator, which is the inverse of the forward kinematics. The solution to the forward kinematics problem is simple and unique, whereas the solution to the inverse kinematics problem is complex and may have multiple solutions or no solutions at all. Factors that affect the finishing accuracy of a robotic arm include kinematic interpolation, arm load, stiffness, mechanical clearance, tool wear, and thermal effects. An important way to improve the positioning accuracy is to establish a positioning compensation algorithm and an error model. The positioning accuracy of the robotic arm can be divided into two categories: absolute positioning and repeatable positioning accuracy. The absolute positioning accuracy refers to the deviation between the set value and the actual value, and the repeated positioning accuracy refers to the position deviation when the robot arm repeatedly reaches a certain point. Since the repeatable positioning accuracy of robotic arms is generally higher than absolute accuracy, technological breakthroughs in absolute accuracy are particularly important. For this purpose, parameters such as joint stiffness, position error, and temperature deformation of the robot arm need to be identified, an error model or error matrix should be obtained, and the position of the end effector should be servo-corrected. Feedback channels are incorporated into robotic arm servo control, and robotic arm vision servo is one of the methods. The robotic arm visual servo control uses visual feedback sensors to obtain changes in the working environment and image feature extraction through vision processing to obtain the position of the target and the end of the robotic arm in Cartesian space, then the decision control compares the current feedback information with the target information and calculates the corresponding control command to finally guide the robotic arm to complete the task. Through the precision correction algorithm, the 6-axis industrial manipulator system is essentially a semiclosed control structure, which precisely controls the position of the servo motor joint, and the relationship between the motor position and the end effector of the manipulator is determined by kinematics. The relationship between the motor position and the robotic arm end effector position is determined by kinematics. To improve the absolute accuracy of the robotic arm positioning, calibration is necessary because errors inevitably occur between the theoretical kinematics model and the actual model.

In this paper, the posture error model of each joint is constructed and the differential motion model of the overall robot arm is derived by controlling certain joint angles to reduce the effect of singularity.

2.2. Differential Errors in Adjacent Joints. Let $\Delta\theta i$, Δdi, Δai, and $\Delta\alpha i$ represent the error of joint i, which is the final required result. Then, according to the reporter's derivative rule, the differential error transformation matrix between adjacent joints is,

$$
\mathrm{d}A_i = \frac{\partial A_i}{\partial \theta_i}\Delta\theta_i + \frac{\partial A_i}{\partial d_i}\Delta d_i + \frac{\partial A_i}{\partial a_i}\Delta a_i + \frac{\partial A_i}{\partial \alpha_i}\Delta\alpha_i \quad (i = 1, 2, 3, 4, 5, 6), \tag{3}
$$

easy to get

$$
\begin{aligned}
\frac{\partial A_i}{\partial \theta_i} &= \begin{bmatrix} -s\theta_i & -c\alpha_i c\theta_i & s\alpha_i c\theta_i & -a_i s\theta_i \\ c\theta_i & -c\alpha_i s\theta_i & s\alpha_i s\theta_i & a_i c\theta_i \\ 0 & 0 & 0 & 0 \\ 0 & 0 & 0 & 0 \end{bmatrix}, \\
\frac{\partial A_i}{\partial d_i} &= \begin{bmatrix} 0 & 0 & 0 & 0 \\ 0 & 0 & 0 & 0 \\ 0 & 0 & 0 & 1 \\ 0 & 0 & 0 & 0 \end{bmatrix}, \\
\frac{\partial A_i}{\partial a_i} &= \begin{bmatrix} 0 & 0 & 0 & c\theta_i \\ 0 & 0 & 0 & s\theta_i \\ 0 & 0 & 0 & 0 \\ 0 & 0 & 0 & 0 \end{bmatrix}, \\
\frac{\partial A_i}{\partial \alpha_i} &= \begin{bmatrix} 0 & s\theta_i s\alpha_i & s\theta_i c\alpha_i & 0 \\ 0 & -c\theta_i s\alpha_i & -c\theta_i c\alpha_i & 0 \\ 0 & c\alpha_i & -s\alpha_i & 0 \\ 0 & 0 & 0 & 0 \end{bmatrix}.
\end{aligned} \tag{4}
$$

Further, there are

$$
\begin{aligned}
dA_i &= \frac{\partial A_i}{\partial \theta_i}\Delta\theta_i + \frac{\partial A_i}{\partial d_i}\Delta d_i + \frac{\partial A_i}{\partial a_i}\Delta a_i + \frac{\partial A_i}{\partial \alpha_i}\Delta\alpha_i \\
&= A_i\left(\Omega_{\theta i} + \Omega_{di} + \Omega_{ai} + \Omega_{\alpha i}\right) = A_i\Omega_i \quad (i = 1, 2, 3, 4, 5, 6),
\end{aligned} \tag{5}
$$

of which $\Omega_{\theta i} = \begin{bmatrix} 0 & -c\alpha_i & s\alpha_i & 0 \\ c\alpha_i & 0 & 0 & a_i c\alpha_i \\ -s\alpha_i & 0 & 0 & -a_i s\alpha_i \\ 0 & 0 & 0 & 0 \end{bmatrix}$

$$\Omega_{\alpha i} = \begin{bmatrix} 0 & 0 & 0 & 0 \\ 0 & 0 & -1 & 0 \\ 0 & 1 & 0 & 0 \\ 0 & 0 & 0 & 0 \end{bmatrix},$$

$$\Omega_{di} = \begin{bmatrix} 0 & 0 & 0 & 0 \\ 0 & 0 & 0 & s\alpha_i \\ 0 & 0 & 0 & c\alpha_i \\ 0 & 0 & 0 & 0 \end{bmatrix},$$

$$\Omega_{ai} = \begin{bmatrix} 0 & 0 & 0 & 1 \\ 0 & 0 & 0 & 0 \\ 0 & 0 & 0 & 0 \\ 0 & 0 & 0 & 0 \end{bmatrix},$$

$$\Omega_i = \begin{bmatrix} 0 & -c\alpha_i\Delta\theta_i & s\alpha_i\Delta\theta_i & \Delta a \\ c\alpha_i\Delta\theta_i & 0 & \Delta\alpha_i & a_i c\alpha_i\Delta\theta_i + s\alpha_i\Delta d_i \\ -s\alpha_i\Delta\theta_i & -\Delta\alpha_i & 0 & -a_i s\alpha_i\Delta\theta_i + c\alpha_i\Delta d_i \\ 0 & 0 & 0 & 0 \end{bmatrix}. \tag{6}$$

In the above equation, Ω_i is called the error matrix operator.

In contrast, the MDH model yields an error matrix operator of

$$\frac{\partial A_i}{\partial \theta_i} = \begin{bmatrix} -s\theta_i & -c\alpha_i c\theta_i & 0 & 0 \\ c\alpha_i c\theta_i & -c\alpha_i s\theta_i & 0 & 0 \\ s\alpha_i s\theta_i & -s\alpha_i s\theta_i & 0 & 0 \\ 0 & 0 & 0 & 0 \end{bmatrix},$$

$$\frac{\partial A_i}{\partial d_i} = \begin{bmatrix} 0 & 0 & 0 & 0 \\ 0 & 0 & 0 & -s\alpha_i \\ 0 & 0 & 0 & c\alpha_i \\ 0 & 0 & 0 & 0 \end{bmatrix},$$

$$\frac{\partial A_i}{\partial a_i} = \begin{bmatrix} 0 & 0 & 0 & 1 \\ 0 & 0 & 0 & 0 \\ 0 & 0 & 0 & 0 \\ 0 & 0 & 0 & 0 \end{bmatrix},$$

$$\frac{\partial A_i}{\partial \alpha_i} = \begin{bmatrix} 0 & 0 & 0 & 0 \\ -s\theta_i s\alpha_i & -c\theta_i s\alpha_i & -c\alpha_i & -d_i c\alpha_i \\ s\theta_i c\alpha_i & c\theta_i c\alpha_i & -s\alpha_i & -d_i s\alpha_i \\ 0 & 0 & 0 & 0 \end{bmatrix},$$

$$\Omega_i = \begin{bmatrix} 0 & -c\alpha_i\Delta\theta_i & s\alpha_i\Delta\theta_i & -d_i s\theta_i\Delta\alpha_i + c\theta_i\Delta a_i \\ \Delta\theta_i & 0 & -c\theta_i\Delta\alpha_i & -d_i c\theta_i\Delta\alpha_i - s\theta_i\Delta a_i \\ s\theta_i\Delta\theta_i & c\theta_i\Delta\alpha_i & 0 & \Delta d_i \\ 0 & 0 & 0 & 0 \end{bmatrix}. \tag{7}$$

Comparing (6) and (7), it can be found that the error matrix operator of the SDH model is independent of the joint angle θ_i, i.e., when the end position of the arm changes and thus the joints of the arm change, the error matrix operator remains constant, which provides a good condition for the accuracy of the error calibration results and greatly simplifies the operation. The error matrix operator of the MDH model is related to the joint angle θ_i, which brings variability to the subsequent calibration algorithm, so this chapter uses the SDH model for error calibration.

The recursive equation for the differential error of each joint is derived from equation (6).

$$\begin{aligned} dT_1 &= A_1, \\ dT_n &= \prod_{i=1}^{n}(A_i + dA_i) - \prod_{i=1}^{n} A_i \quad (n = 1, 2, 3, 4, 5, 6). \end{aligned} \tag{8}$$

It is obvious that expanding the equation $\mathrm{d}T_n$ to contain multiple $\mathrm{d}A_i$ cross-multiplying terms can be considered as higher-order infinitesimals with respect to $\mathrm{d}A_i$, which can be ignored, and simplifying it further yields

$$\begin{aligned} dT_n &= \sum_{i=1}^{n}(A_1 A_2 \ldots dA_i \ldots A_n) = dT_{n-1} * A_n + T_{n-1} * dA_n \\ &= dT_{n-1} * A_n + T_n * \Omega_n \, (n = 2, 3, 4, 5, 6). \end{aligned} \tag{9}$$

The equations of the error model are thus established. The parameters $\Delta\theta i$, Δdi, Δai, and $\Delta\alpha i$ to be calibrated are contained in the matrix Ω_n and $\mathrm{d}T_6$ is the direct data obtained from the measuring instruments in the experiment.

2.3. Differential Error Model for Inverse Order Joints. In the previous subsection, a recursive formula for the error in the position of the adjacent joints of the robot arm was obtained. Further processing of equation gives the relationship between the error accumulated at joint i and the error in each joint before joint i.

$$\begin{aligned} dT_n * T_n^{-1} &= dT_{n-1} * A_n * T_n^{-1} + T_n * \Omega_n * T_n^{-1} \\ &= dT_{n-1} * T_n^{-1} + T_n * \Omega_n * T_n^{-1} \\ &= \sum_{i=1}^{n} T_i * \Omega_i * T_i^{-1} \, (n = 1, 2, 3, 4, 5, 6). \end{aligned} \tag{10}$$

A closer look at this equation shows that the error at the end of the robot arm $\mathrm{d}T_n * T_n^{-1}$ is in the form of a sum about the parameters of the individual joints, and that their sums are independent of each other and no coupling terms appear, which provides the preconditions for the elimination method.

It can be seen that T_i is the transformation matrix of joint $i-1$ to joint i, i.e., $T_i = \begin{bmatrix} R_i & p_i \\ 0 & 1 \end{bmatrix}$, $\Omega_i = \begin{bmatrix} Q_i & l_i \\ 0 & 0 \end{bmatrix}$. Therefore, we have $T_i \Omega_i T_i^{-1} = \begin{bmatrix} R_i Q_i R_i^{-1} & -R_i Q_i R_i^{-1} p_i + R_i l_i \\ 0 & 0 \end{bmatrix} = \begin{bmatrix} R_i Q_i R_i^{T} & -R_i Q_i R_i^{T} p_i + R_i l_i \\ 0 & 0 \end{bmatrix}$ and note that $R_i Q_i R_i^T$ is an antisymmetric matrix whose elements are opposite to each other after corresponding along the main diagonal, which greatly reduces the number of equations and thus achieves the effect of reducing the rank of the coefficient matrix.

According to the characteristics of equations (3)–(13), the first $n-2$ joints can be controlled so that their joint angles remain constant and only the joint angle n and joint angle $n-1$ are changed so that the matrix equations for θn, d_n, a_n, α_n, $\theta_n - 1$, $d_n - 1$, $a_n - 1$, and $\alpha_n - 1$ can be obtained as follows:

$$\begin{aligned} \left[dT_n * T_n^{-1}\right]' - \left[dT_n * T_n^{-1}\right]'' &= D_n = W_n \\ &= \left[T_n * \Omega_n * T_n^{-1}\right]' \\ &\quad - \left[T_n * \Omega_n * T_n^{-1}\right]''. \end{aligned} \tag{11}$$

Due to the SDH singularity, the coefficient matrices of $\theta_n - 1$, $d_n - 1$, $a_n - 1$, and $\alpha_n - 1$ are close to singular values, so the calibration results of the structural parameters of joints $n-1$ $\theta_n - 1$, $d_n -$, $a_n - 1$, and $\alpha_n - 1$ are discarded and only the experimental results of θ_n, d_n, a_n, and α_n are retained. In the above equation, $[\,]'$ and $[\,]''$ represent the two sets of measurements, respectively, D represents the matrix obtained from the measurements, i.e., the expression on the left side of the equation, and W represents the result obtained by numerical calculation, i.e., the expression on the left side of the equation.

$$W_n = \begin{bmatrix} 0 & W_n(1,2) & W_n(1,3) & W_n(1,4) \\ -W_n(1,2) & 0 & W_n(2,3) & W_n(2,4) \\ -W_n(1,3) & -W_n(2,3) & 0 & W_n(3,4) \\ 0 & 0 & 0 & 0 \end{bmatrix}, \text{and.} \tag{12}$$

The following is an example of how to solve for the structural parameters θ_6, d_6, a_6, and α_6 for the last joint calibrated, i.e., the 6th joint.

To simplify the calculation, it is assumed that the value of α in the SDH model can only be taken to two common parameter values, 0 and $\pm\pi/2$. The error matrix equation of (10), which is an equation for the joint angle n and the joint angle $n-1$, can be calculated as follows:

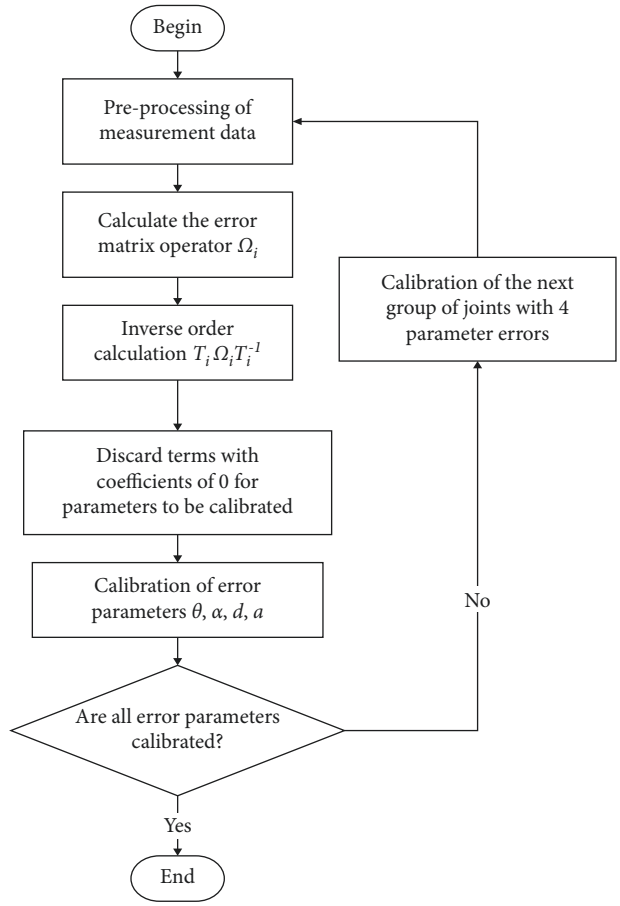

Figure 2: Flow chart of the calibration algorithm.

$$
\begin{aligned}
W_6(1,2) &= (f_{12}f_{21}c\alpha - f_{13}f_{21}s\alpha - f_{11}f_{22}c\alpha + f_{11}f_{23}s\alpha)\Delta\theta + (f_{13}f_{22}s\alpha - f_{12}f_{23}s\alpha)\Delta\alpha \\
&= -f_{33}\Delta\theta - f_{31}\Delta\alpha, \\
W_6(1,3) &= (f_{12}f_{31}c\alpha - f_{13}f_{31}s\alpha - f_{11}f_{32}c\alpha + f_{11}f_{33}s\alpha)\Delta\theta + (f_{13}f_{32}s\alpha - f_{12}f_{33}s\alpha)\Delta\alpha \\
&= f_{23}\Delta\theta + f_{21}\Delta\alpha, \\
W_6(2,3) &= (f_{22}f_{31}c\alpha - f_{23}f_{31}s\alpha - f_{21}f_{32}c\alpha + f_{21}f_{33}s\alpha)\Delta\theta + (f_{23}f_{32}s\alpha - f_{22}f_{33}s\alpha)\Delta\alpha \\
&= -f_{13}\Delta\theta - f_{11}\Delta\alpha, \\
W_6(1,4) &= f_{24}(f_{33}\Delta\theta + f_{31}\Delta\alpha) + f_{34}(f_{23}\Delta\theta + f_{21} + \Delta\alpha) + f_{11}\Delta a + f_{12}a\Delta\theta + f_{13}\Delta d \\
&= (f_{24}f_{33} + f_{34}f_{23} + f_{12}a)\Delta\theta + (f_{24}f_{31} - f_{34}f_{21})\Delta a + f_{13}\Delta d + f_{11}\Delta a, \\
W_6(2,4) &= f_{14}(f_{33}\Delta\theta + f_{31}\Delta\alpha) + f_{34}(f_{23}\Delta\theta + f_{21} + \Delta\alpha) + f_{21}\Delta a + f_{22}a\Delta\theta + f_{23}\Delta d \\
&= (-f_{14}f_{33} + f_{34}f_{13} + f_{22}a)\Delta\theta + (-f_{14}f_{31} - f_{34}f_{11})\Delta a + f_{23}\Delta d + f_{21}\Delta a, \\
W_6(3,4) &= f_{14}(f_{33}\Delta\theta + f_{31}\Delta\alpha) + f_{24}(f_{23}\Delta\theta + f_{21} + \Delta\alpha) + f_{31}\Delta a + f_{32}a\Delta\theta + f_{33}\Delta d \\
&= (f_{14}f_{23} - f_{24}f_{13} + f_{32}a)\Delta\theta + (f_{14}f_{21} + f_{24}f_{11})\Delta a + f_{33}\Delta d + f_{31}\Delta a.
\end{aligned} \tag{13}
$$

According to the characteristics of the SDH transformation matrix, the first three equations in equation can be calibrated to $\Delta\alpha_6$ and Δa_6. After the calculation of equation (9), the coefficients before $\Delta\theta_5$ and Δd_5 are close to zero and can be neglected, and finally a matrix equation is obtained for $\Delta\theta_6$, Δd_6, Δa_6, $\Delta\alpha_6$, Δa_5, and $\Delta\alpha_6$, so that the coefficient

Table 1: SDH parameter table.

Coordinate system i	θ (rad)	d (mm)	a (mm)	α (rad)	Offset angle offset
1	q_1	0	160	$-\pi/2$	0
2	q_2	0	580	0	$-\pi/2$
3	q_3	0	200	$-\pi/2$	0
4	q_4	640	0	$\pi/2$	0
5	q_5	228	0	$-\pi/2$	0
6	q_6	0	0	0	0

Note. The offset angle is the initial rotation angle of the joint and remains constant during the calibration process.

Table 2: Comparison of the calibration results between the least-square method and the method in this paper.

Joint	Structural error parameters	Traditional methods	Methodology of this paper
1	$\Delta\theta 1$ (rad)	0.00533251466	0.0053513684
	$\Delta\alpha 1$ (rad)	−0.00304622132	−0.0030531436
	$\Delta a1$ (mm)	0.04655832461	0.0426131686
	$\Delta d1$ (mm)	0.03632714664	0.0365462379
2	$\Delta\theta 2$ (rad)	0.00795465466	0.0079457325
	$\Delta\alpha 2$ (rad)	0.00346976216	0.0035372149
	$\Delta a2$ (mm)	−0.04672446465	−0.0464634195
	$\Delta d2$ (mm)	0.07986544668	0.0794546871
3	$\Delta\theta 3$ (rad)	0.00625973164	0.0062458734
	$\Delta\alpha 3$ (rad)	0.00354361779	0.0035704687
	$\Delta a3$ (mm)	−0.03672479864	−0.0646795362
	$\Delta d3$ (mm)	0.02673468355	0.0269664734
4	$\Delta\theta 4$ (rad)	0.00254346944	0.0025095875
	$\Delta\alpha 4$ (rad)	−0.00386434867	−0.0038144762
	$\Delta a5$ (mm)	0.03489742168	0.0344986135
	$\Delta d5$ (mm)	0.03179612134	0.0313465435
5	$\Delta\theta 5$ (rad)	0.00379643685	0.0038745186
	$\Delta\alpha 5$ (rad)	0.00296120547	0.0029486467
	$\Delta a5$ (mm)	0.03798613486	0.0374644675
	$\Delta d5$ (mm)	−0.05153420564	−0.0575135439
6	$\Delta\theta 6$ (rad)	0.00272526803	0.0027892526
	$\Delta\alpha 6$ (rad)	0.00364679616	0.0036670627
	$\Delta a6$ (mm)	0.02604359755	0.0267691487
	$\Delta d5$ (mm)	0.05345746395	0.0532546387

matrix is not a singular matrix and can be directly calculated to obtain $\Delta\theta_6$, Δd_6, Δa_6, and $\Delta\alpha_6$. The flow chart of the algorithm is shown in Figure 2.

For the error parameters of joints 5, 4, 3, 2, and 1, new measurement data can be collected and calculated by (11) to obtain

$$W_i = W_{i+1} * {}_i^{i+1}T^{-1} \ (i = 2, 3, 4, 5). \tag{14}$$

3. Simulation Experiments and Verification Results

The SDH parameters of the robotic arm used in this paper are shown in Table 1.

Experiments were performed using open-loop measurements, where an external measurement device was used to measure the position of an end-mounted actuator or actuator. For each calibration, two measurements are taken for each joint i. A total of $5 \times 2 = 10$ sets of data are selected to ensure that the joint angles, except joint i and joint $i-1$ remain unchanged so that only the differential transformation information of joint i is preserved after they are substracted. In this loop, the error matrix is calculated and the parameters are calibrated until all parameters are calibrated. In the experimental process, the method in this paper is compared with the ordinary least-square method, which reduces the computational complexity and improves the real-time performance of the system while ensuring calibration accuracy. The data used for comparison are shown in Table 2.

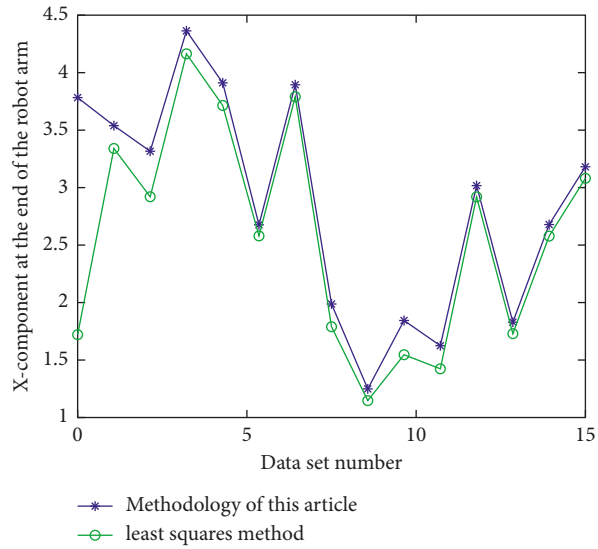

Figure 3: Comparison of errors in the x-component.

As can be seen from Table 2, in terms of calibration accuracy, the method in this paper is not inferior to the common least-square method, but in terms of the process of calculating the calibration error, the least-square method has to find the pseudo-inverse of a coefficient matrix of order 4×6 to obtain the solution of the chi-square linear equation. In contrast, the method in this paper obtains the final calibration results by computing five 6×6 full rank matrices after further transformation of the error equation, which greatly simplifies the calculation.

In the course of the experiments, the results of the calibration were compensated for errors with the aid of the inspection data set, and the differences in position at the end of the robotic arm were obtained by comparing the method of this paper with the least-square method, as shown in Figures 3–5.

The horizontal coordinates of the above three plots represent the number of the inspection data set, and the vertical coordinates represent the deviation of the end position of the robot arm under the two methods. The calculation method is as follows: the 6 data of each set represent 6 joint angles, which are substituted into (1) and (2) to obtain ${}_0^6T$. The results are then substituted into (5) and (8) to obtain the error differential matrix after compensation.

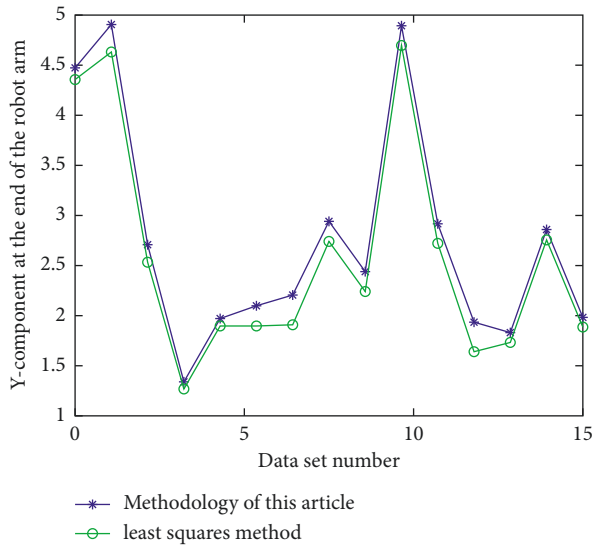

Figure 4: Comparison of errors in the y-component.

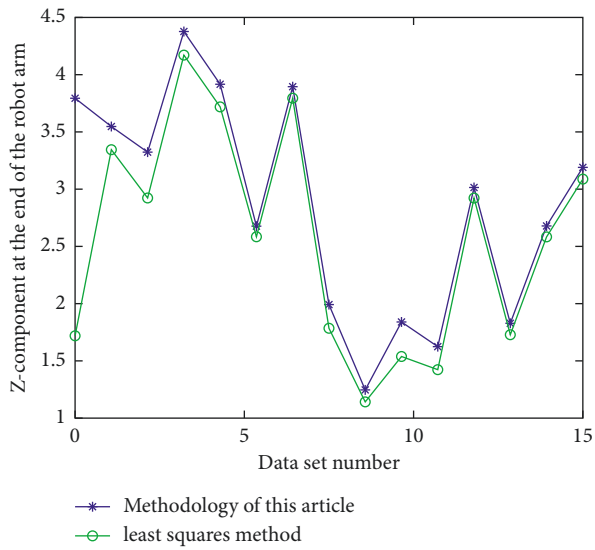

Figure 5: Comparison of errors in the z component.

From the results in the figure, we can see that the calibration method in this paper is slightly better than the common least-square method, which again verifies the feasibility and effectiveness of the method in this paper. At the same time, due to the small volume of measurement data collected in this paper, the inverse process of a large matrix is decomposed into the inverse process of several small matrices, which greatly simplifies the calculation and reduces the time cost.

Figure 6 shows a comparison of the least-square method and the differential elimination method proposed in this chapter in terms of calibration time; the differential elimination method takes almost half the time, and the time spent is more stable.

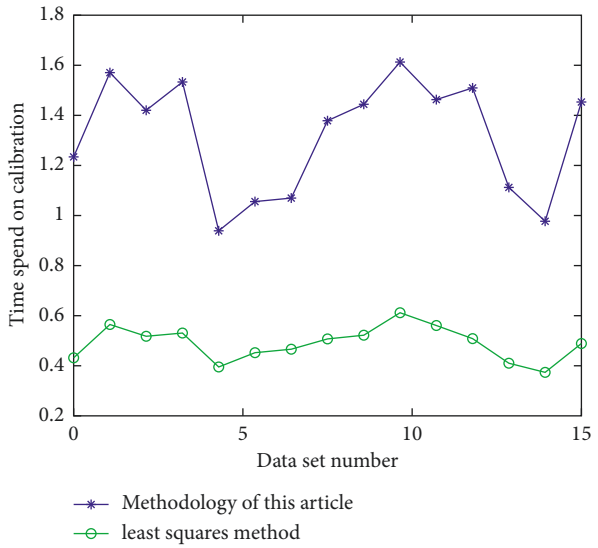

Figure 6: Comparison of the times of the two methods.

4. Conclusion

In this paper, an error calibration optimization method based on the SDH model is proposed by analyzing the composition of the transformation matrix and according to its characteristics. This method solves the singularity problem of the SDH model in the application of calibration error. It is not only better than the traditional calibration method and least-square method in terms of calibration accuracy but also realizes simple calculation by discarding some abnormal calibration values. Finally, through the verification of simulation experiments, it is proved that this method can be used to identify the error of the model parameters of the manipulator and achieve the desired effect. The source of error is not only the structural parameters of the arm but also many external factors. The calibration accuracy of this method is improved when compared to the least-square method, but it is still in the same order of magnitude and does not significantly improve the calibration accuracy, so it cannot be used in demanding working environments. These aspects will also be further investigated in future research work. Because the method in this paper has high requirements on the posture of the manipulator, it reduces the overall calibration calculation and saves time, which has a certain effect on the improvement of the industrial manipulator in the manufacturing industry.

Data Availability

The data used to support the findings of this study are available from the corresponding author upon request.

Conflicts of Interest

The authors declare that they have no conflicts of interest.

Acknowledgments

This research study was sponsored by the National Natural Science Foundation of China; the name of the project is National Natural Science Foundation of China Grant (Project no. 31370565). The authors thank the project for supporting this article.

References

[1] B. Wu and H. Li, "Unfixed-standard visual servo with a new image Jacobian estimation method," *System Simulation Journal*, vol. 20, no. 14, pp. 3767–3771, 2018.

[2] X. Jing, L. Ding, and Y. Yang, "A new calibration-free self-disturbance visual servo control method for double-loop robot," *Robot*, vol. 29, no. 1, pp. 35–40, 2017.

[3] J. Zhao, Li Mu, and Li Ge, "Research on a non-calibration visual servo control technique," *Control and Decision-Making*, vol. 21, no. 9, pp. 1015–1019, 2019.

[4] Z. Guo, S. Chen, and L. Wu, "An image-based calibration-free visual servo method," *Harbin Industrial University Journal*, vol. 34, no. 3, pp. 294–296, 2019.

[5] Z. Gao and J. Su, "Image Jacobian estimation method with delay compensation," *Control Theory & Applications*, vol. 26, no. 1, pp. 23–27, 2019.

[6] K. Pan, J. Su, and Y. Xi, "Neural network-based robotic hand-eye uncalibration plane visual tracking," *Acta Automatica Sinica*, vol. 27, no. 2, pp. 194–199, 2021.

[7] L. Ding, X. Liu, and Y. Yang, "Robot-free hand-eye coordination based on genetically optimized self-disturbance controller," *Machine Man*, vol. 28, no. 5, pp. 510–514, 2016.

[8] M. Xue and X. Ren, "Adaptive tracking control of the calibration-free visual robotic arm based on task space," *Control and decision-making*, vol. 28, no. 7, pp. 1060–1064, 2018.

[9] J. Su, "Application and development of ADRC theory and technology in robotic calibration-free visual servo," *Control and decision-making*, vol. 30, no. 1, pp. 1–8, 2019.